

Hopping conduction and random telegraph signal in an exfoliated multilayer MoS₂ field-effect transistor

Lijun Li¹, Inyeal Lee¹, Doo-Hyeob Youn² and Gil-Ho Kim¹

¹ School of Electronic and Electrical Engineering and Sungkyunkwan University Advanced Institute of Nanotechnology, Sungkyunkwan University, Suwon 16419, Korea

² ICT Components and Materials Technology Research Division, Electronics and Telecommunications Research Institute, Daejeon 34129, Korea

E-mail: ghkim@skku.edu

Received 14 September 2016, revised 11 December 2016


Accepted for publication 15 December 2016

Published 13 January 2017



Abstract

We investigate the hopping conduction and random telegraph signal caused by various species of interface charge scatterers in a MoS₂ multilayer field-effect transistor. The temperature dependence of the channel resistivity shows that at low temperatures and low carrier densities the carrier transport is via Mott variable range hopping with a hopping length changing from 41 to 80 nm. The hopping conduction was due to electron tunneling through localized band tail states formed by the scatterers located in the vicinity of the MoS₂ layer. In the temperature range of 40–70 K, we observed random telegraph signal (RTS) that is caused by the capture and emission of a carrier by the interface traps that are located away from the layer. These traps form strong potential that interact with the layer and change the potential profile of the electron system. The characteristics of RTS depend strongly on gate bias and temperature, as well as the application of a magnetic field.

 Online supplementary data available from stacks.iop.org/nano/28/075201/mmedia

Keywords: MoS₂ multilayer field effect transistor, variable range hopping, random telegraph signal

(Some figures may appear in colour only in the online journal)

MoS₂ is a typical material belonging to the family of transition metal dichalcogenides that had attracted a great deal of interests for the application in nanoelectronics. Theoretical predictions and experimental observations have demonstrated that atomic thin layers of MoS₂ manifest striking electrical and optical properties [1–4]. Because of the large effective mass and valley degeneracy, back-gated multilayer MoS₂ devices are usually operating as a non-degenerate semiconductor, where screening of Coulomb scatterers is very weak or even absent. For field-effect transistors (FETs) made by layer transfer on the required substrate the interface scatterers play important roles in the performance of the device [5]. Even in high quality devices that are encapsulated by

boron nitride manifesting quantum Hall effect [6], the interface scattering centers introduced by the transfer process can still exist³. These scattering centers when located in the very vicinity of the layer form localized band tail states where carrier transport is via hopping conduction. When these scatterers are sparsely populated and located with a slightly larger distance from the layer because of the substrate roughness or corrugation of the layer, they can form a strong scattering potential with a tunneling barrier to the electron

³ We have observed RTS in a boron nitride encapsulated few layer MoS₂ field-effect transistor that shows quantum Hall effect with mobility 3000 cm² V⁻¹ s⁻¹. Data will be presented elsewhere.

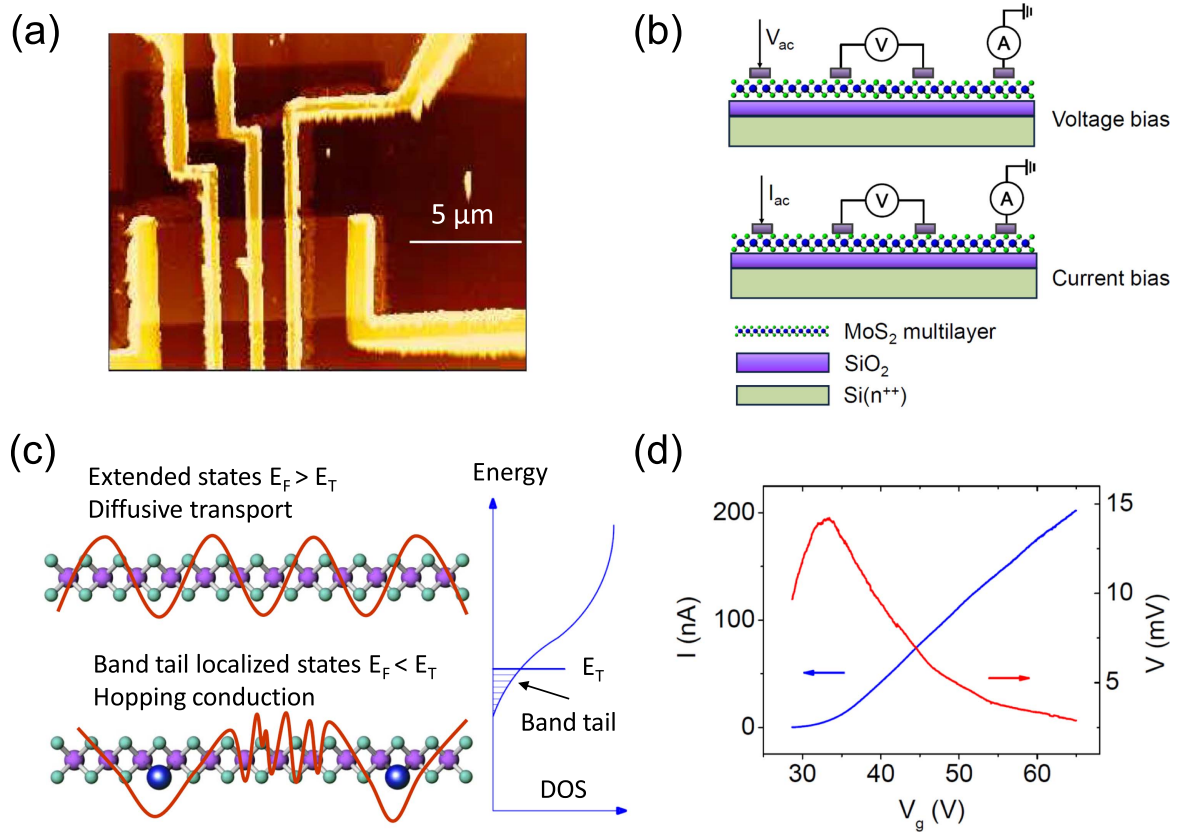


Figure 1. (a) An AFM image of the device. (b) The measurement layout with voltage bias and with current bias. The voltage bias method was applied in gate sweeps. The fixed current method was used in the measurement of random telegraph signal in magnetic field. (c) The schematics of band structure of disordered semiconductor with a band tail. When the Fermi level lies in the band tail, the electronic states are localized and the carrier transport is by hopping conduction. (d) An example of gate sweep measurement results at 40 K.

system and produce random telegraph signal (RTS) characterized by discrete resistance fluctuations in small devices due to the exchange of a charge with the electron system through tunneling [7]. It is believed that the superposition of many of these capture and emission events gives rise to the $1/f$ noise [7]. RTS has been observed in various structures including Si inversion layers, GaAs split gate device, and more recently in carbon nanotube FETs [8–13], but not in devices made by atomic layer transition metal dichalcogenides yet. In this work we research the electrical property of a multilayer MoS₂ FET at low temperatures. We shall discuss the contact behavior and reexamine the previously reported metal insulator transition (MIT) and hopping conduction [14–17]. Furthermore, we shall discuss our observations of the RTS that manifests in voltage/current measurements in our device.

The device was a multilayer MoS₂ on SiO₂ substrate with Co electrodes. Result of the Raman shift shows that the thickness is likely to be five layers. Details of the fabrication and Raman results are presented in section I of supplementary material. After packed into a chip carrier the sample surface was coated with Poly(methyl methacrylate) (PMMA) with an aim to protect the device from contamination of air. Figure 1(a) shows the atomic force microscope (AFM) image of the device without PMMA on it. Measurement was performed in a helium flow cryostat with lock-in amplifiers. The

measurement schematics were shown in figure 1(b). In the voltage bias method, a voltage was applied to the outer two contacts, while the current I flowing through the channel and the voltage drop V on the two inner contacts are simultaneously measured. In the current bias method, a fixed current was applied through the outer two contacts and the voltage drop V on the inner two contacts was measured. Figure 1(d) shows the typical curves of gate dependent I and V at 40 K measured with voltage bias method. In this way we can investigate the channel electrical property and the contribution from the contact resistance.

First we look at the contact resistance of the device. Using the field emission theory we have obtained a negative barrier height as the gate bias was varied from 35 to 65 V (see details in figure S2 in supplementary material). The negative value means that the Schottky barrier does not exist and thermionic emission description of the contact behavior is not valid [18]. In this circumstance the contact resistance is Ohmic. This result is different from previous works that observed considerable barrier height of MoS₂ device with Co direct contact [19, 20]. We thought that the Ohmic behavior of Co contact in our device is due to the effect of annealing. We have also observed Ohmic behavior from a bilayer MoS₂ device with Ti/Au electrodes annealed at same conditions with the present device [21]. We thought that it is possible that annealing makes the metal to diffuse into MoS₂ and form

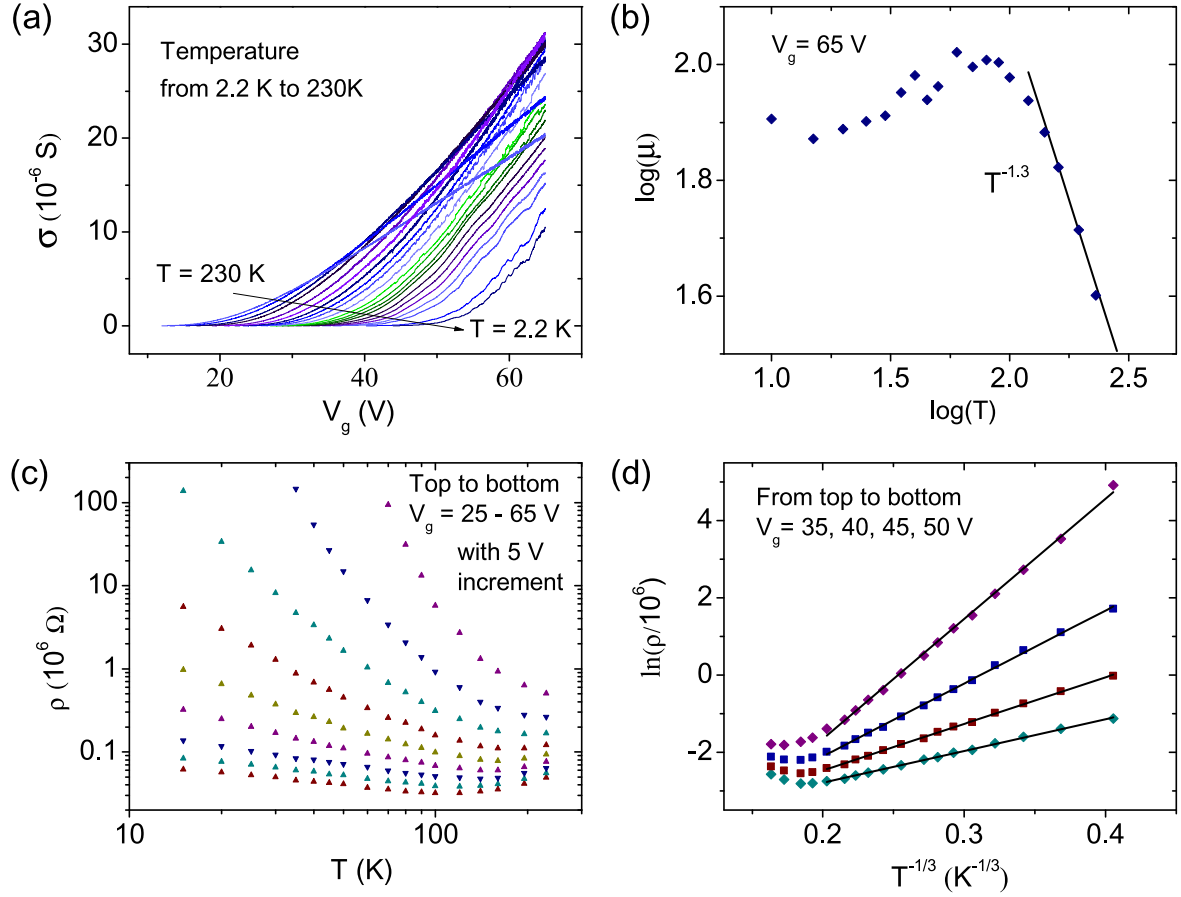


Figure 2. (a) Gate effect of σ at various temperatures of 2.2, 4.2, 10, 15, 20, 25, 30, 35, 40, 45, 50, 60, 70, 80, 90, 100, 120, 140, 160, 195, and 230 K. (b) Temperature dependent mobility at $V_g = 65$ V. The slope shows $\mu \sim T^{-1.3}$. (c) ρ plotted as a function of temperature at various V_g . (d) Temperature dependence of the resistivity follows Mott variable range hopping conduction at $T < 100$ K. Symbols are experimental results, lines are linear fit to obtain the T_0 value.

a thin layer of alloy. To prove this further characterization is needed and we leave for future investigations.

In figure 2(a) conductivity σ was plotted with sweeping gate bias at temperatures from 2.2 to 230 K. There is a crossing area of the σ at around 100 K. At $V_g = 65$ V, $T > 100$ K, the temperature dependence of the field effect mobility shows a $T^{-1.3}$ dependence (figure 2(b)). At specific gate biases the temperature dependence of the resistivity ρ was plotted in figure 2(c). There is a turning point in the $\rho \sim T$ curves around 100 K at high V_g values. Similar behavior had been reported in mono- and multilayers and was designated as MIT [14, 15]. We thought that this finite temperature dependence is not a genuine effect of MIT. We believe that at high temperature region, the contribution from phonons affects more on the temperature dependence of ρ than the contribution from the localization mechanism in a disordered conductor that render the material an insulator. At lower temperatures, the phonon contribution is wiped out and this ‘metallic’ behavior disappears. The temperature dependence of the mobility ($T^{-1.3}$) also reveals the contribution from phonon effect [6, 22, 23].

We estimated the carrier density from $\sigma = en\mu$ at 100 K and found $n = 2.0 \times 10^{12} \text{ cm}^{-2}$ at $V_g = 65$ V, it decreases to $9.4 \times 10^{11} \text{ cm}^{-2}$ at $V_g = 50$ V. At V_g values lower than 50 V,

the conductance curve deviates from the linear character and relation $\sigma = en\mu$ loses its validity. Next we examine the electrical property at low carrier densities and low temperatures. In figure 2(d) we plotted the logarithm of ρ as a function of $T^{-1/3}$. The linear dependence reveals that in this temperature range the conduction is via variable range hopping, $\rho \sim \exp(T_0/T)^{1/3}$, here $T_0 = \frac{\beta_M}{g_0 \xi^2}$. $\beta_M = 13.8$, ξ is the localization length and g_0 is the localized density of states. In a disordered semiconductor, when the Fermi level lies in the band tail, the carrier wave function is localized around defect/impurity sites and carrier transport shows hopping conduction (See schematics in figure 1(c)). Sulfur vacancies, which were considered to be responsible for the localized states that give rise to hopping conduction in MoS₂ in previous report [16] are not the defect species making the decisive effect in our device. Using the same source material, our boron nitride encapsulated MoS₂ multilayers show much higher mobility and quantum hall effect at low temperature (see footnote 3). The most important scattering centers in this device may include the gaseous adsorbates between the layer and the substrates (here the substrate means SiO₂ or PMMA), and other kind of interface scatterers like dangling bonds at the SiO₂ surface [5]. Using the surface density of states

Table 1. The hopping parameter T_0 , localization length ξ , and hopping length l_H at various V_g . l_H was calculated at 10 K.

V_g (V)	T_0 (K)	ξ (nm)	l_H (nm)
35	3.0×10^4	8.6	41
40	6.8×10^3	18	52
45	1.8×10^3	36	67
50	5.6×10^2	63	80

$g_0 = 7.2 \times 10^{12} \text{ eV}^{-1} \text{ cm}^2$ as the localized density of states [24], parameters T_0 , ξ and hopping length l_H were calculated and presented in table 1. T_0 spans three orders of magnitude from 560 K at 50 V to 3.0×10^4 at 35 V. ξ changes from 8.6 nm at 35 V to 63 nm at 50 V. At 10 K, l_H is 41 nm at 35 V, and 80 nm at 50 V.

We have calculated parameter r_s [25], the ratio of Coulomb energy to Fermi energy, by expression

$$r_s = \frac{g_v}{a_B \sqrt{\pi n}} = \frac{g_v m^* e^2}{4\pi \epsilon \hbar^2 \sqrt{\pi n}} \quad (1)$$

where g_v is the valley degeneracy, a_B is the effective Bohr radius, m^* is the electron effective mass, ϵ is the dielectric constant of the bulk MoS₂ and \hbar the reduced Planck constant. Using the electron density calculated from 100 K and values $m^* = 0.82m_e$ [26], $\epsilon = 7.6\epsilon_0$ [27, 28], $g_v = 6$ in multilayer MoS₂, the obtained r_s changes from 48 at $V_g = 65$ V to 71 at $V_g = 50$ V. Because of the large effective mass and large valley degeneracy in MoS₂, the r_s values are much larger than those in GaAs heterostructures with similar electron density [29]. Next we estimate the value of $k_F l$, the criterion of the strength of disorder [30], where $k_F = \sqrt{2\pi n}/g_v$ is the Fermi wave vector and $l = \hbar k_F \mu / e$ is the electron mean free path. $k_F l$ values are much smaller than 1 in our sample, it changes from 0.14 at $V_g = 65$ –0.065 V at $V_g = 50$ V. At $T \leq 60$ K, $V_g = 65$ V, and 60 V, the temperature dependence of ρ follows $\rho \sim \ln T$ (see supplementary figure S3). At low temperatures both weaklocalization (WL) and electron–electron interaction (EEI) correction to conductivity suggest a logarithmic temperature dependence [31, 32]. Consider that there is no magnetoresistance, WL effect can be ruled out [31, 33]. The EEI correction also gives rise to a magnetoresistance, but the correction part is proportional to $(1 - \mu^2 B^2) \delta\sigma^{ee}(T)$, here $\delta\sigma^{ee}(T)$ is the zero field EEI correction. With the largest $\mu \sim 100 \text{ cm}^2 \text{ V}^{-1} \text{ s}^{-1}$, $\mu^2 B^2 \sim 0.0025$ at 5 T. Thus the change in ρ from magnetic field correction is too small to be measured [34].

We have discussed the hopping conduction caused by scattering centers located in the vicinity of the channel. When there are interface charge traps located somewhat away from the channel, and the energy of the traps are aligned close to the Fermi level of the channel, they can capture and emit carriers and give rise to RTS. Study of the RTS is useful to find out the nature of the charge traps such as the polarity and the energy state, so that improvement of the device performance can be achieved by an optimization of the fabrication process. We observed RTS in the gate sweeping measurement in the temperature range of 40–70 K. The magnitude of the

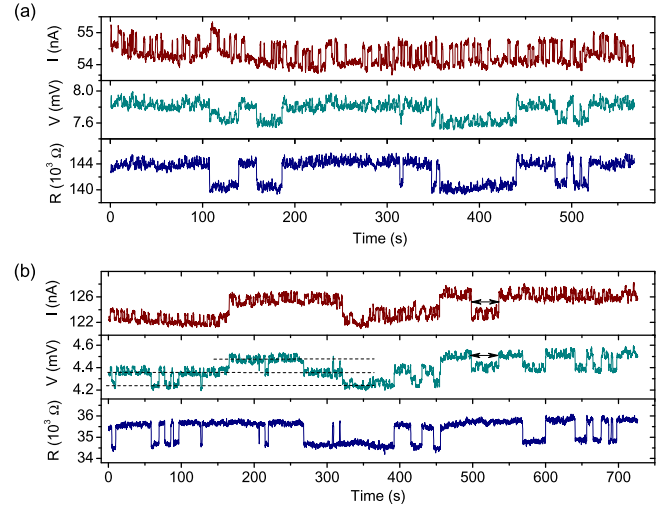


Figure 3. RTS in current and in voltage and in calculated resistance measured by voltage bias method at 50 K, $V_g = 40$ V (a), and 50 V (b). Note in (b) the voltage has three levels that are illustrated by dashed lines; the simultaneous change with current does not show in resistance. See the change in current and in voltage indicated by black arrows having no contribution to the resistance.

level change fell in the range of 1%–3%. The gate dependent σ curves showing RTS were replotted in supplementary figure S4. From 40 K, σ starts to show the discrete levels. With increasing temperature the frequency of the level change becomes faster. At 80 K the discrete levels can not be seen. The two discrete conducting states were caused by carrier trapping and de-trapping from defect sites located in the interface between the MoS₂ and SiO₂ substrate, or, between the MoS₂ and the coated PMMA. These interface defects could be gaseous adsorbates that were formed in device fabrication process. In this temperature range the capture and emission of a charge carrier that gives rise to RTS is usually caused by thermally activated behavior mediated by multiphonon processes [7, 35]. The defect traps that cause the RTS are likely to be interface defects such as adsorbates or dangling bonds, but different in character in terms of location and energy from those that form the localized states in hopping conduction. In circumstances that RTS appears, the defect traps are sparsely populated in a spacial position somewhat away from the conducting channel and brings a variation in potential and an effective change in the doping level of the channel.

We first measured the RTS at varies temperatures and gate voltages with the voltage bias method. At $T = 50$ K, data of RTS with $V_g = 40$ and 50 V were presented in figures 3(a) and (b). At $V_g = 40$ V, in the current signal, there are two well defined discrete levels. In the voltage signal, an in-phase change with current exists together with a much slower change of itself. The in phase signal does not make contribution to the resistance. At $V_g = 50$ V, the two levels in the current signal becomes less refined and a slow change in current also appears; in the voltage signal three levels develops (see the dashed lines in middle panel of figure 3(b)). The calculated resistance has two levels but having different pattern from current. The current signal changes faster with

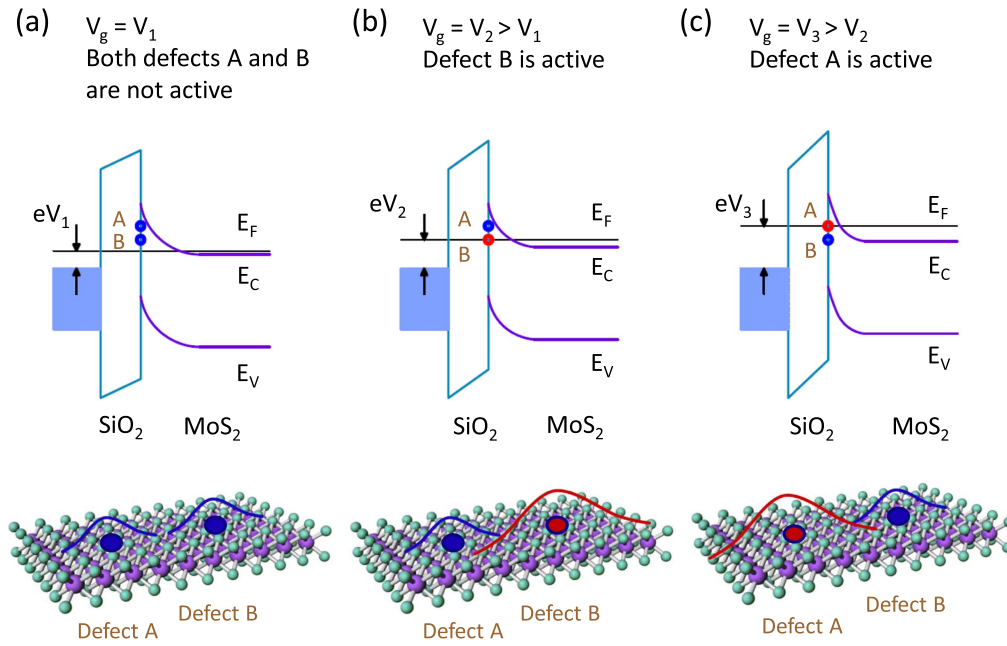


Figure 4. Schematics showing that the RTS caused by the interface defect has dependence on gate bias. (a) When E_F is far away from the energy levels of the defects, they are not active. (b) and (c) when E_F is close to one of the energy levels of A or B, the relevant defect becomes active.

smaller magnitude about 1%; the resistance change is much slower with larger magnitude of 2%–3%. At higher V_g , the resistance change becomes faster (compare the lower panel in figures 3(a) and (b)). As T increases to 60 K, the current signal has two finely defined discrete levels, but in the voltage signal, three levels with similar characteristics developed (figure 5(b)). At this temperature, the level change in resistance is much faster than that in 50 K. The level change magnitudes in current and in resistance are similar $\sim 2\%$ – 3% at 60 K. The signals are qualitatively the same when V_g was varied from 48 to 52 V (figure 5(a)).

Now we focus on the fast RTS in current at 50 K. From the mean of the two current level dwell time, i.e., the capture time and emission time, τ_1 and τ_2 (for this purpose, we collected data containing 100–140 periods of each level), the energy difference, ΔE , of the defect states with or without a trapped carrier was calculated by $\frac{\tau_1}{\tau_2} = \exp(-\frac{\Delta E}{k_B T})$. Precisely ΔE bears the meaning of total difference of free energy of the two states with or without a charge trapped in the defect site [35–37]. ΔE consists two parts: the Coulomb energy ΔE_C , and the energy difference between the Fermi level and the defect trap level E_{TF} . Varying V_g brings a change in E_{TF} obviously, in addition the Fermi level change brings a change in ΔE_C because of the interaction between the defects and the electron wave function [38], brought by the Friedel oscillations of the electron density around the defect site [39]. ΔE is 3.5 meV at $V_g = 40$ V and 2.1 meV at $V_g = 50$ V. These energies correspond to 41 K and 25 K, respectively. When V_g is varied by 10 V, the change of Fermi level is 0.34 meV, which is much smaller than the magnitude of ΔE . We consider that the RTS measured from $V_g = 40$ – 60 V is produced by the same traps. From the V_g dependence of τ_1 and τ_2 , we deduce that both the traps measured by current and by voltage

are positive in the absence of trapping of an electron [9]. At 60 K, ΔE in the current was estimated to be 4.0 meV at $V_g = 48$ V (in this case data containing more than 80 periods of each level were collected), and in resistance ΔE is 3.0 meV. With the limit of our data we can not definitely say that the RTS features in current and in voltage are caused by the same or by different kind of impurities at 60 K. From the change of ΔE in 50 and 60 K, it is likely that the current measures different defects but the voltage may measure the same kind of defects.

The V_g dependence of RTS caused by the interface defects are illustrated in the simplified picture in figure 4. As V_g is more positively biased, the Fermi level moves up and approaches the E_{TF} of defect B, and defect B becomes active. With V_g increased further, the Fermi level leaves E_{TF} of B and approaches E_{TF} of A, and defect A becomes active. In circumstances that two defects have close values of E_{TF} and their spatial separation fell in the effective range of the Friedel oscillations, the two defects could become correlated. The RTS feature in current curves of figure 3(b) showing more than two discrete levels are caused by two defects with the slow one makes strong variation of potential of the channel. The magnitude and trapping time of the fast signal does not show an effect of modulation from the slow one. We can come to the conclusion that the two defects are not correlated [40, 41]. With the slow feature in current having a magnitude comparable to the RTS in resistance, a question arises whether the slow RTS and resistance belong to the same defect. We explain the different characteristics of RTS observed in current and in resistance in figure 3 with different measuring sensitivity in different areas because of the presence of the metal electrodes. The RTS in resistance measures the capture and emission events in sample area

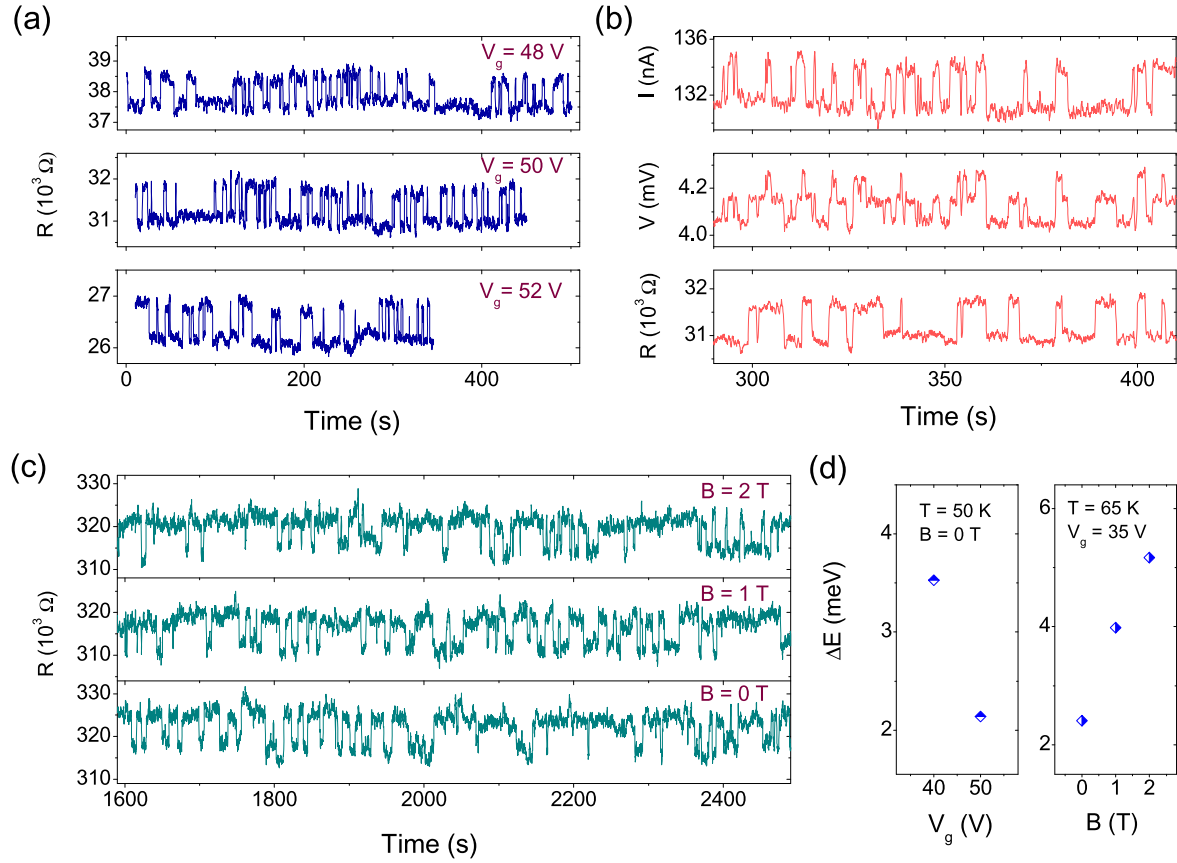


Figure 5. (a) The resistance RTS at 60 K, $V_g = 48, 50$, and 52 V. (b) The current, voltage and calculated resistance RTS at 60 K, $V_g = 50$ V. Note that the current signal shows two discrete levels, the voltage signal shows three levels. The calculated resistance has two levels. (c) RTS in resistance measurement at fixed current of 10.5 nA in a perpendicular magnetic field. From lower to upper $B = 0, 1$, and 2 T. (d) The gate and magnetic field dependence of the two state energy difference.

($4.6 \times 1.5 \mu\text{m}$) enclosed by the inner two electrodes, while the RTS observed in current measures events in the sample area ($4.6 \times 5.7 \mu\text{m}$) enclosed by the outer two contacts. Imagine that defect A and B are close in energy; A resides within the voltage probes, and B outside. The carrier trapping behavior of B is measured by current. The effective region of potential produced by defect B does not extend to the area enclosed by voltage probes, thus the voltage does not measure the state of B, but the voltage simultaneously measures a change with current level. The simultaneous change of voltage with current does not bring a RTS in resistance. A typical example of this was indicated in figures 3(a) and (b) by black arrows. The voltage measures the state of A; the current is not sensitive to the condition of A possibly because of the presence of the electrodes brings a modification to the potential of the electron channel. Therefore, the resistance measures the behavior of defect A.

To investigate the magnetic field effect on the RTS, we measured the RTS at $B = 0, 1$, and 2 T using current bias method at $T = 65$ K, $V_g = 35$ V. (figure 5(c)). These measurements were performed after the device was warmed up to 260 K and cooled down again to 65 K. ΔE has the value of 2.4 meV, 4.0 meV and 5.2 meV at 0 T, 1 T and 2 T, respectively (right panel in figure 5(d)). This magnetic field dependence of ΔE does not suggest that the tunneling

between the defect and the MoS_2 channel is related to the electron spin. Using the value of Lande g factor $g = 1.86$ in MoS_2 [42], the spin split energy is calculated to be 0.11 meV and 0.22 meV at $B = 1$ and 2 T. These energies are one magnitude smaller than the change in ΔE . The absence of any measured magnetoresistance at perpendicular field suggests that the change in ΔE is not related to the Co electrodes. We have discussed in the previous paragraph that in a disordered conducting channel, the local electron density is a function of the space coordination because of the interference of the waves scattered by the specific impurities or defects. The application of a magnetic field changes the conditions of this interference, which results in the readjustment of the local electron density at a specific space coordination, and the modification of the energy configuration of the defect at the site [38]. Magnetic field dependence of ΔE in RTS had been previously observed in metal structures [8], and in Si FETs [10, 43]. The presence of the RTS is not expected in transistor applications. Our results show that thermal cycling have effect on the RTS. After warming up to 260 K and cooled down to 65 K, The RTS at 35 V is still very obvious, but at higher V_g , RTS disappeared.

In conclusion we have investigated the carrier transport in an exfoliated multilayer MoS_2 field-effect transistor. Our results show that the interface scattering centers have

important effect in the electrical properties of the device. At low temperatures and low carrier densities the carrier conduction is via Mott variable range hopping through localized states formed by interface scattering centers that are located in the vicinity of the layer. When sparsely populated interface charge traps located in a position away from the MoS₂, we observe random telegraph signal caused by carrier tunneling between the MoS₂ layer and the defect sites. The energy difference of the system when the defect was filled or empty changes with carrier density and the application of a magnetic field through the re-normalization of defect energy configuration by the electron wave function.

Acknowledgements

This research was supported by the Basic Science Research Program through the National Research Foundation of Korea (NRF) funded by the Ministry of Education, Science and Technology (2016R1A2A2A05921925), and the Institute for Information and Communications Technology Promotion (IITP) grant funded by the Korea government (MSIP) (B0117-16-1003, Fundamental technologies of two-dimensional materials and devices for the platform of new-functional smart devices). We are thankful to Sung Ho Jhang for valuable discussions and comments.

References

- [1] Costanzo D, Jo S, Berger H and Morpurgo A F 2016 *Nat. Nanotechnol.* **11** 339–44
- [2] Xiao D, Liu G-B, Feng W, Xu X and Yao W 2012 *Phys. Rev. Lett.* **108** 196802
- [3] Yuan H *et al* 2013 *Nat. Phys.* **9** 563–9
- [4] Amani M *et al* 2015 *Science* **350** 1065–8
- [5] Li S-L, Wakabayashi K, Xu Y, Nakaharai S, Komatsu K, Li W-W, Lin Y-F, Aparecido-Ferreira A and Tsukagoshi A 2013 *Nano Lett.* **13** 3546–52
- [6] Cui X *et al* 2015 *Nat. Nanotechnol.* **10** 534–40
- [7] Kirton M J and Uren M J 1989 *Adv. Phys.* **38** 367–468
- [8] Zimmerman N M, Golding B and Haemmerle W H 1991 *Phys. Rev. Lett.* **67** 1222–325
- [9] Ralls K S, Skocpol W J, Jackel L D, Howard R E, Fetter L A, Epworth R W and Tennant D M 1984 *Phys. Rev. Lett.* **52** 228–31
- [10] Cobden D H and Muzykantskii B A 1995 *Phys. Rev. Lett.* **75** 4274–7
- [11] Cobden D H, Savchenko A, Pepper M, Petal N K, Ritchie D A, Frost J E F and Jones G A C 1992 *Phys. Rev. Lett.* **69** 502–5
- [12] Pioro-Ladriere M, Davies J H, Long A R, Sachrajda A S, Gaudreau L, Zawadzki P, Lapointe J, Gupta J, Wasilewski Z and Studenikin S 2006 *Physica E* **34** 553–6 arXiv:cond-mat/0503602v2
- [13] Sharf T, Wang N-P, Kevek J W, Brown M A, Heinze S and Minot E D 2014 *Nano Lett.* **14** 4925–30
- [14] Park M J, Yi S-G, Kim J H and Yoo K-H 2015 *Nanoscale* **7** 15127–33
- [15] Radisavljevic B and Kis A 2013 *Nat. Mat.* **12** 815–20
- [16] Qiu H *et al* 2013 *Nat. Commun.* **4** 2642
- [17] Ghatak S, Pal A N and Ghosh A 2011 *ACS Nano* **5** 7707–12
- [18] Rhoderick E H and Williams R H 1988 *Metal–Semiconductor Contact* (Oxford: Clarendon)
- [19] Chen J R, Odenthal P M, Swartz A G, Floyd G C, Wen H, Luo K and Kawakami R K 2013 *Nano Lett.* **13** 3106–10
- [20] Dankert A, Langouche L, Kamalakar M V and Dash S P 2014 *ACS Nano* **8** 476–82
- [21] Li L, Lee I, Lim D, Kang M, Kim G-H, Aoki N, Ochiai Y, Watanabe K and Taniguchi T 2015 *Nanotechnology* **26** 295702
- [22] Baugher B W H, Churchill H O H, Yang Y and Jaarillo-herrero P 2013 *Nano Lett.* **13** 4212–6
- [23] Kaasbjerg K, Thygesen K S and Jacobsen K W 2012 *Phys. Rev. B* **85** 115317
- [24] Ayari A, Cobas E, Ogundadegbe O and Fuhrer M S 2007 *J. Appl. Phys.* **101** 014507
- [25] Das Sarma S, Adam S, Hwang E H and Rossi E 2011 *Rev. Mod. Phys.* **83** 407–70
- [26] Yun W S, Han S W, Hong S C, Kim I G and Lee J D 2012 *Phys. Rev. B* **85** 033305
- [27] Ma N and Jena D 2014 *Phys. Rev. X* **4** 011043
- [28] Kim S *et al* 2012 *Nat. Commun.* **3** 1011
- [29] Allison G, Galaktionov E A, Savchenko A K, Safonov S S, Fogler M M, Simmons M Y and Ritchie D A 2006 *Phys. Rev. Lett.* **96** 216407
- [30] Lee P A and Ramakrishnan T V 1985 *Rev. Mod. Phys.* **57** 287–337
- [31] Lin B J F, Paalanen M A, Gossard A C and Tsui D C 1984 *Phys. Rev. B* **29** 927–34
- [32] Minkov G M, Rut O E, Germanenko A V, Sherstobitov A A, Zvonkov B N, Uskova E A and Birukov A A 2002 *Phys. Rev. B* **65** 235322
- [33] Li L, Wang J, Kim G-H and Ritchie D A 2012 *J. Phys.: Condens. Matter* **24** 385301
- [34] Li L, Proskuryakov Y Y, Savchenko A K, Linfield E H and Ritchie D A 2003 *Phys. Rev. Lett.* **90** 076802
- [35] Palma A, Godoy A, Jimenez-Tejada J A, Carceller J E and Lopez-Villanueva J A 1997 *Phys. Rev. B* **56** 9565–74
- [36] Shulz M 1993 *J. Appl. Phys.* **74** 2649–57
- [37] Mueller H H, Wörle D and Schulz M 1994 *J. Appl. Phys.* **75** 2970–9
- [38] Altshuler B and Spivak B Z 1989 *JETP Lett* **49** 772–6 http://www.jetpletters.ac.ru/ps/1123/article_17018.pdf/article_17018.pdf
- [39] Ruden A M, Aleiner I L and Glazman L I 1997 *Phys. Rev. B* **55** 9322–5
- [40] Farmer K R, Rogers C T and Buhrman R A 1987 *Phys. Rev. Lett.* **58** 2255–8
- [41] Ralls K S and Buhrman R A 1988 *Phys. Rev. Lett.* **60** 2434–7
- [42] Yang L, Chen W, McCreary K M, Jonker B T, Lou J and Crooker S A 2015 *Nano Lett.* **15** 8250–4
- [43] Xiao M, Martin I and Jiang H W 2003 *Phys. Rev. Lett.* **91** 078301